***Original Research Article***

# The biosorption features of Cr (VI) ions by dried biomass of a facultative anaerobic *Bacillus cereus* strain Pf-1


## Abstract

Many studies were undertaken on the biosorption potential of different kinds of biomaterials. However, there is a paucity of data regarding the biosorption mechanism of Cr (VI) using dried cells. In our study, the removal of Cr (VI) from aqueous solution was investigated in a batch system by the dried biomass of a chromium-resistant bacterium isolated from activated sludge samples. Equilibrium and kinetic experiments were undertaken at various initial metal concentration, pH, and biosorbent dosage. *Bacillus cereus* biomass was characterized using Energy-Dispersive X-ray (EDX), Scanning Electron Microscope (SEM) and Fourier Transform Infrared Spectroscopy (FTIR). Biosorption process was found to be pH dependent. The optimum pH was found to be 2.0. The Langmuir and Freundlich were considered to identify the isotherm that could better describe the equilibrium adsorption of Cr (VI) onto the biomass. Langmuir and Freundlich models fitted our experimental data. The suitability of the pseudo-first order and pseudo-second order kinetic models for the biosorption of Cr (VI) onto *Bacillus cereus* was also performed. The mechanism for the adsorption was studied by fitting the kinetic data with the Boyd plot and intra-particle diffusion model. External mass transfer was found to be the rate-determining step. Based on the ionic nature of the metal, the intra-particle diffusion and extent of film diffusion varied.

**Keywords**: Pf-1 strain, biosorption, Langmuir, Cr (VI), biomass

## 1. Introduction

Release of large quantities of heavy metals into the natural environment has resulted in a number of environmental problems. Constituting one of the major causes of environmental pollution, chromium, in hexavalent form [Cr (VI)], is one of the most toxic heavy metal and has become a serious health concern (Nguema et al., 2014). Although some metals are necessary for biological processes, all of them are toxic at high concentrations. This is due to their oxidative capacity to form free radicals and their ability to replace essential metals in enzymes, interrupting their normal activity (Velasquez and Dussan 2002; Nguema et al., 2014). Non-essential metals are very toxic even at low concentration and can be accumulated in different organisms. Chromium in the hexavalent form is toxic, mutagenic and carcinogenic to animals as well as humans and is associated with decrease plant growth and change in plant morphology (Bennett et al. 2013). Biosorption of metal is an example of a wide variety of potential and actual applications of bioremediation technique in wastewater treatment (Fernandez et al., 2017).

*Bacillus cereus* is a facultative anaerobic, gram-positive bacterium, commonly used in many microbiological tests. As a common soil/activated sludge bacterium, *Bacillus cereus* is well adapted for growth in the intestinal tract of insects and mammals (Stenfors et al. 2008). Different studies in the field of bioremediation were conducted with different strains of *Bacillus cereus*, suggesting that *Bacillus cereus* could be used as a target microorganism in the bioremediation of heavy metals in the environment (Giri et al. 2013; Fernandez et al., 2017).

Conventional removal of Cr (VI) from the environment involves expensive physico-chemical treatments generating secondary waste that adds to the problem (Srivastava and Thakur 2006). Biological systems employing processes such as bioreduction, bioaccumulation or biosorption with living cells have been extensively examined for their Cr removal abilities (Fernandez et al., 2017; Fernandez et al., 2018).

Previous studies have been reported in this context employing a wide variety of microorganisms like fungi, algae, protozoa, and bacteria. Among the microorganisms, bacteria are better candidate as they can be easily cultured with simple nutrients and ease to handle (Nguema et al., 2014; Nemr et al., 2015; Mahmoud and Mohamed, 2015; Huang et al., 2016)). Biosorption is a passive process which utilizes the cell wall of biomass to sequester the Cr (VI) ions from aqueous solutions. The mechanisms of cell surface sorption are independent of cell metabolism which is based on physico-chemical interactions between the metal and functional groups of the cell wall. The cell wall of a microorganism mainly consists of polysaccharides, lipids, and proteins that serve as binding sites for metals. Further, this biological approach is cost effective and is considered to be a green technology (Bennett et al. 2013; Fernandez et al., 2018).

Microbial cells, either living or dead biomasses, are effective biosorbents of soluble and particulate heavy metals via their cell wall surfaces which act as sites for metal in attachment. With the inception of microbial bioremediation, this study may be of future use in removing Cr (VI) from the environment. Once complete removal of Cr (VI) from the environment has been achieved, cleaner and metal-free water and soil systems will be obtained and preserved for future generations. Many results have been documented on the biosorption ability of *Bacillus cereus*

biomass to remove heavy metal ions from aqueous solution. However, limited studies reported the metal biosorption potential using dried biomass.

In the present study, the main objective was to investigate the biosorption characteristic of Cr (VI) by using dried biomass of *Bacillus cereus* Pf-1 strain in aqueous solution. First of all, we determined the optimum conditions (pH, sorbent dosage, and Cr (VI) concentration) for the maximum biosorption yield for Cr (VI), secondly we explored the biosorption mechanisms of the sorbent in terms of equilibrium, isotherms and kinetics studies, and finally we characterized the *B. cereus* biomass using SEM-EDX and FTIR imaging.

## 2. Materials and methods

### a. Biosorbent

Pure culture previously isolated from activated sludge sample was grown on Nutrient Broths medium (NB) previously sterilized (121˚ C for 15 min), the pH was adjusted to 7.0±0.03 with 10% (W/v) NaOH or 10% (V/v) HCL solutions and the reaction was incubated at 30˚ C under orbital shaking (100rpm). After 24 h of incubation, cells were collected by centrifugation (10,000 ×g for 5 min), washed three times with phosphate buffer (pH 7.2), dried in oven at 80˚ C for 24 h (Model DHG-9240A), crushed in a blender, sieved through a 24-mesh sieve (Velasquez and Dussan 2002). Samples were stored in a tight container for further use.

### b. Experiments

#### i. Effects of biosorption conditions

The experiments were carried out in a set of Erlenmeyer flasks (250 mL) by shaking desired amount of biosorbent powder in 100 mL Cr (VI) solutions as potassium dichromate ($K_2Cr_2O_{7)}$ of

desired concentrations, pH, and temperature to reach equilibrium of the solid-solution mixture. Samples were pelletized in a centrifuge at 10,000 × g for 5 min and the supernatants were essayed for residual Cr (VI) concentration by 1, 5-diphenylcarbazide spectrophotometric method (DPC) measuring the absorbance at 540 nm by using a spectrophotometer (WFZ800-D3B UV/VIS spectrophotometer) (APHA 1995).

Effect of pH was studied by adjusting the initial pH of Cr (VI) solutions using diluted hydrochloric acid (HCL) or sodium hydroxide (NaOH) solutions (pHs 1, 2, 3, 4, 5, and 6), and the solutions were agitated with 0.02 g/L sorbent dose for 10 mg Cr (VI)/L at 30˚ C.

Four Cr (VI) concentrations (10, 20, 40, and 80 mg/L) were used for the study of initial concentration effect on the biosorption at 30˚C.

Effect of biosorption dosage was studied with different sorbent doses (0.02, 0.05, and 0.1g) and 100 mL of 10 mg Cr (VI)/L solutions at the favorable pH (2.0) and temperature (30º C).

ii. kinetics

Kinetic studies were carried out in a set of 250 mL Erlenmeyer flasks at 30˚C, by shaking 0.02 g/L sorbent powder in 100 mL Cr (VI) solutions (10, 20, 40, and 80 mg/L) in each capped flask at the stirring speed of 100 rpm. The aqueous samples were taken from different flasks at different time intervals of 15, 30, 60, 120, 240, 420, 720, and 1,440 min respectively. All the samples were centrifuged as mentioned above, and the remaining Cr (VI) concentrations in aqueous solution were determined by DPC method. The amount of adsorbed Cr (VI) by the bacterial cells was calculated by the concentration difference method based on the mass balance of the metal ions expressed as (Sivasamy and Sundarabal 2011):

$$q_t = \frac{V(C_0 - C_f)}{X} \quad (1)$$

Where $q_t$ is the specific metal uptake (mg /g), $V$ is the liquid sample volume (mL), $C_0$ is the initial concentration of the metal in the solution at time $t_0$ = 0 h (mg/L), and $C_f$ is the final concentration of the metal in the solution at time $t = t$ (min) and $X$ the amount of added bio sorbent on the dry basic (g). At the sorption equilibrium, $C_f$ equals the equilibrium concentration of the metal ion in the solution ($C_e$, mg/L) ant $q_t$ equals metal sorption uptake or equilibrium bio-sorption capacity of Cr (VI) ($q_e$, mg/g).

For each sorption experiment, a control set containing only Cr (VI) solution of appropriate concentration was kept. All the experiments were conducted in triplicate and repeated twice.

### iii. isotherms

Biosorption experiments were performed in a set of 100 mL Erlenmeyer flasks, where solutions of Cr (VI) with different initial concentrations (10, 20, 40, and 80 mg/L) were placed. Equal masses of 0.02 g/L biosorbent were added to Cr (VI) solutions, and each sample was kept in 30˚C at a stirring speed of 100 rpm for 1,440 min each to reach equilibrium of the solid-solution mixture. The flaks were then removed from the rotary shaker, and the final Cr (VI) concentration in the solution was analyzed as mentioned above. A control set without biomass was kept and triplicate experiments were also kept and repeated twice. The statiscal software package Origin Pro 8.0 was used for regression analysis of experimental data

### c. FTIR analysis

Infrared spectroscopic analysis for the biomass under investigation was performed in order to give a qualitative and preliminary characterization of the main functional chemical groups on the

bacterial biomass which could be responsible for Cr (VI) biosorption. Infrared spectra of biomasses before and after biosorption were obtained on a FTIR (Thermo Fisher Scientific China, Nicolet 6700). The biomass/KBr mass ratio used for the preparation of the disks was 1:200. They were ground into fine powder and compressed into translucent sample disk using a manual hydraulic press at a pressure of 100kg/cm$^2$. The disk was then fixed in FTIR and the spectrum was obtained at a single scan. The shifts in the FTIR peaks were determined with references to reported standard values (Samuel et al. 2012).

d. SEM-EDX analysis of the sample

Cells were fixed in glutaraldehyde (1%) and paraformaldehyde (2%) buffered with sodium phosphate buffer saline (0.1M, pH 6.8) for 12-18h at 4º C after which cells were washed in fresh buffer and then fixed for 2h in osmium tetraoxide (1%) in the same buffer at 4º C. The bacterial cells fixed were smeared with poly-L-lysine for 30 min in wet condition. The specimen was washed with phosphate buffer and then dehydrated in a series of ethanol-water solution (30%, 50%, 70% and 90% ethanol, 5 min each) and dried under $CO_2$ atmosphere for 20 min. Mounting was done on aluminum stubs, and cells were coated with 90Å thick gold-palladium coating in polar on Sc 7640 sputter coater (VG Microthech, East Sussex, TN22, England) for 30 min. coated cells were viewed at 20kV with scanning electron microscopy (Model-Zeiss EVO40). Energy dispersive X-ray spectrometer (EDAX, USA) was performed at 5kV for confirming the biosorption of chromium in the bacterial cell. X-ray absorption spectroscopy provides information on the electronic and structural state of an element (Srivastava and Thakur 2007; Samuel et al., 2012).

## 3. Results and discussion

149 a. Characterization of Pf-1 strain biomass

150 The surface morphology of the biomass without and with the sorption of Cr (VI) ions during bio
151 sorption process was measured with the help of SEM-EDX, and the results were shown in Fig. 1.
152 Without sorption of Cr (VI) ions, Pf-1 strain cells were rod-shaped, elongated and the presence
153 of elements such as carbon, phosphorus, potassium, sulfate, magnesium, sodium, aluminum,
154 chloride, and oxygen on the surface of the biomass (Fig. 1a). Through ionic exchange
155 interactions, these elements could affect the sorption process. It could be clearly observed that
156 the biomass shape and the amount and type of elements present in the biomass were considerably
157 changed (Fig. 1b). Bacterial cells became small, round-shaped with uneven edges on cell wall.
158 These changes in the amount and type of elements present in the biomass confirm that the
159 sorption has taking place. However, the Cr peak (5.5 keV) was observed only in treated sample
160 and which also confirms the adsorption of Cr (VI) onto the biomass. It has been reported that,
161 with progressive increase in chromium concentration, the cell becomes both longer and wider.
162 However, further increase in chromate led to decrease in cell size (Naik et al. 2012). The process
163 of uptake and retention of the heavy metals by the cell wall of *Bacillus* sp. has also been studied
164 with the help of EDX analysis (Beveridge and Murray 1980; Naik et al., 2012).

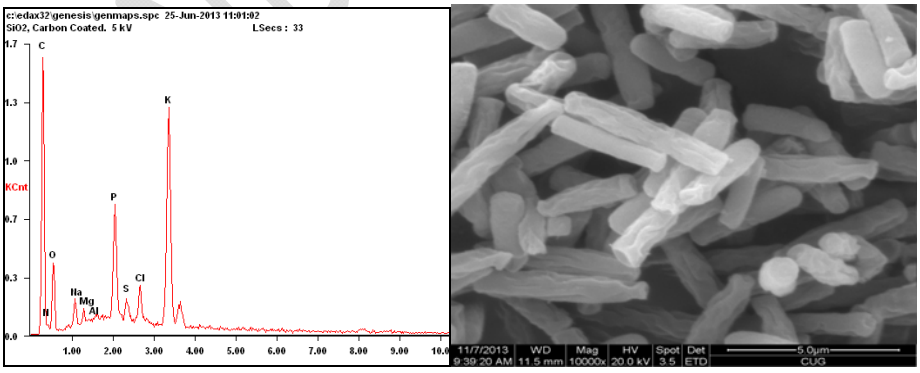


165

166 **Fig.1a**: SEM-EDX images of *Bacillus cereus* without sorption of Cr (VI) ions

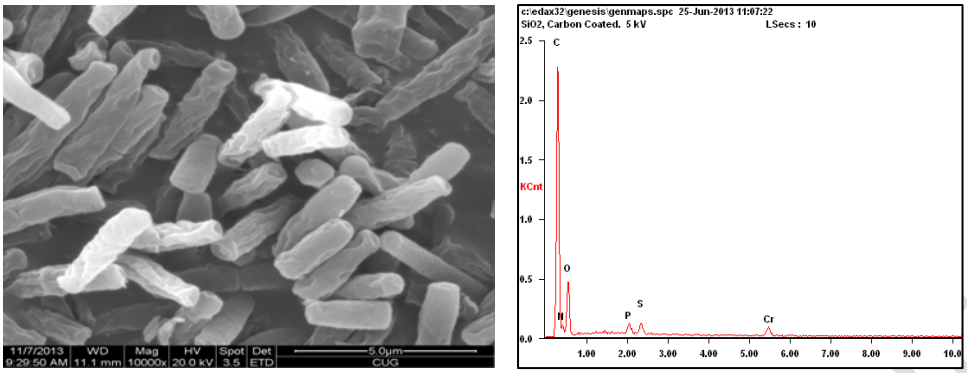


167

168 **Fig.1b**: SEM-EDX images of *Bacillus cereus* with sorption of Cr (VI) ions

169 b. FTIR analysis of PF-1 strain biomass

170 The FTIR spectra of the *B. cereus* biomass with and without Cr (VI) ions loaded which were
171 obtained to determine the probable functional groups which may have contributed to the Cr (VI)
172 ions sorption were presented in (Table 1). The FTIR spectra of *B. cereus* biomass in the control
173 display a number of absorption peaks, indicating the complex nature of the bacterial biomass.
174 The spectra of loaded and unloaded Cr (VI) ions were compared and a shift was found. The
175 spectra of sorbent exhibit a broad absorption band at 3,065.66 $cm^{-1}$ due to bonded O-H and N-H
176 groups which is shifted to 2,964.54 $cm^{-1}$ which might be possibly due to the complexation of
177 amino groups of proteins and water representing hydration heavy metal (Mishra and Doble 2008).
178 The absorption peaks at 1,742.04 $cm^{-1}$ due to bonded O-H group stretching from aliphatic ester is
179 shifted to 1,743.56 $cm^{-1}$ (Mishra and Doble 2008). The peak at 1,538.78 $cm^{-1}$ has been shifted at
180 a lower frequency to 1,528.13 $cm^{-1}$, possibly due to the complexation of amide group (N-H
181 stretching and C=O stretching vibration) with Cr (VI) ions (Qing et al. 2007). The peak at
182 1,401.16 $cm^{-1}$ was disappeared after the sorption was taking place. Another shift to a lower

frequency was observed from 1,069.99 $cm^{-1}$ to 1,056.70 $cm^{-1}$ due to the interaction of nitrogen from the amino group with Cr (VI) ions may be attributed to the C-N stretching vibrations of amino groups (Giri et al., 2011). The phenomenon of biosorption on the bacterial cell surface might be occurring due to the modification of functional groups. So, the functional groups like carboxyl, amide, and hydroxyl groups were likely to be responsible for the biosorption of chromium and help in detoxification process. The chromium binding sites were mostly carbonyl and amide groups (Kang et al., 2006). Role of negatively charged COOH groups of the yeast for the absorption of metal like Pb has been studied through FTIR analysis (Ashkenazy et al. 1997). Generally, heavy metals affect its bio-specific interaction with the expression and suppression of certain functional groups on bacterial cell wall which might help the bacterial strain to tolerate the toxicity of the heavy metals (Kamrev 2008).

Table 1: characteristic biosorption bands of Cr (VI) unloaded/loaded *B. cereus* biomass

| Suggested assignment | Unloaded biomass frequency ($cm^{-1}$) | Loaded biomass frequency ($cm^{-1}$) |
|---|---|---|
| -OH, -CH and –NH stretching | 3,065.66 | 2,964.54 |
| -OH stretching | 1,742.04 | 1,743.56 |
| -NH and C=O stretching | 1,538.78 | 1,528.13 |
| -COO- anions band | 1,401.16 | - |
| -C-O and –C-N stretching | 1,069.99 | 1,056.70 |

### c. Effects of biosorption conditions

#### i. Effects of pH

As the initial pH increased (1 - 6), the biosorption capacity and the corresponding removal efficiency decreased (Fig. 2). The maximum sorption capacity was observed at pH 2. The main predominant form of Cr (VI) is the acid chromate ions species, $HCrO_4^-$ at lower pH solution and subsequently $HCrO_4^-$ shifted to other forms, $CrO_4^{2-}$ and $Cr_2O_7^{2-}$ as increasing pH. At lower pH, due to the excess amount of $H^+$ within the medium, the active sites on the adsorbent become positively charged. This causes a strong attraction between these sites and negatively charged $HCrO_4^-$ ions. As a result, adsorption of negative metals increases significantly. When pH value increases, surface of the adsorbent becomes neutral and biosorption reduces. When the adsorbent surface is negatively charged, adsorption decreases significantly. This behavior is specific to Cr (VI) and it is different for the divalent metals. Chromium ions release hydroxide ions to the solution instead of proton. This result also agrees with previous studies of Cr (VI) biosorption by different biosorbent (Abbas et al. 2008; Rabei et al. 2009; Aliabadi et al. 2012; Fernandez et al., 2018).

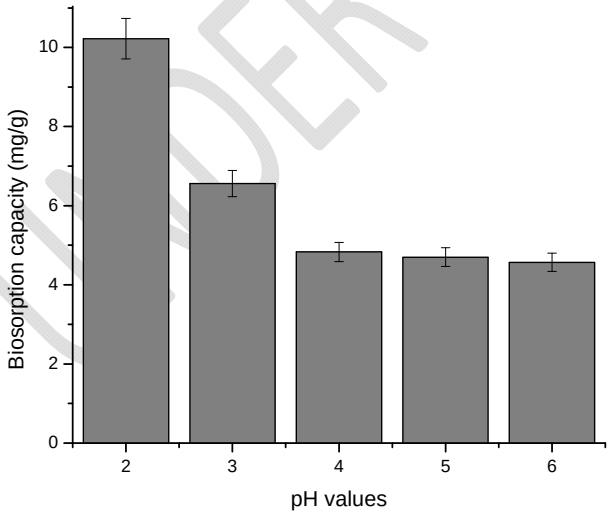

**Fig. 2:** Effect of pH on Cr (VI) biosorption (initial Cr (VI) concentration 10 mg/L, contact time 1,440 min, temperature 30º C, agitation speed 100 rpm, biomass dosage 0.05 g/L)

### ii. Effects of initial metal ion concentrations and sorbent doses

When the initial concentration of Cr (VI) varied (10 - 80 mg/L), the sorption capacity of Pf-1 strain biomass was increased (16 - 86 mg/g) at the sorbent dosage of 0.02g/L (Table 2). In the contrast, at the same initial concentration of Cr (VI) ions, the adsorption efficiency was decreased (31-22 %). The increase of loading capacities of the sorbents with the increase of metal ion concentration is probably due to higher interaction between metals ions and each of sorbent (Mufedah and Sarita 2012; Reya et al. 2012; Nguema et al., 2014). Increase in biosorption efficiency with biosorbent dose can be attributed to increase bio-sorbent surface area and availability of more biosorption sites, but the biosorptive capacity decreased with increase in the biosorbent dose. This can be attributed to overlapping or aggregation of bio-sorbent surface area available to Cr (VI). Additionally, the active site of sorbent will reach the adsorption saturation after a certain time at different sorbent doses. This saturation time depends on the type of biomass and the conditions of the pretreatment. Similar conclusions were found in the literature (Zhu et al. 2012; Reya et al., 2012).

**Table 2:** equilibrium adsorbed quantities of Cr (VI) ions obtained at different initial metal ion concentration and different sorbent dosage (Ad%: adsorption efficiency; $C_0$: initial Cr (VI) concentration, $q_e$: equilibrium sorption capacity; SE: standard error)

| Sorbent (g/L) | | |
|---|---|---|
| 0.02 | 0.05 | 0.1 |

| $C_0$ (mg/l) | $q_e$ (mg/g) ± SE | *Ad%* | $C_0$ (mg/l) | $q_e$ (mg/g) | Ad% | $C_0$ (mg/l) | $q_e$ (mg/g) | *Ad%* |
|---|---|---|---|---|---|---|---|---|
| 10 | 16±0.38 | 31 | 10 | 10±0.28 | 51 | 10 | 7±0.11 | 67 |
| 20 | 24±0.24 | 24 | 20 | 17±0.15 | 44 | 20 | 10±0.10 | 51 |
| 40 | 46±0.33 | 23 | 40 | 27±0.31 | 34 | 40 | 17±0.15 | 38 |
| 80 | 86±0.33 | 22 | 80 | 46±0.22 | 28 | 80 | 29±0.22 | 36 |

231

232 ### iii. kinetics

233 In order to investigate the mechanism of sorption, we have chosen the most commonly use
234 kinetic models namely, the pseudo-first order equation and the pseudo-second order equation.
235 Intra-particle diffusion model and Boyd plot were also investigated.

236 #### 1. Pseudo-first order kinetic model

237 The equation corresponding to the pseudo-first-order kinetic model is the following differential
238 form used by (Zhu et al. 2012):

239 $$\frac{dq_t}{dt} = K_1(q_e - q_t) \qquad (2)$$

240 Integrating this for boundary conditions $q_e = 0$ at $t = 0$ and $q_t = q_t$ at $t = t$, gives:

241 $$\ln\frac{q_e}{q_e - q_t} = K_1 t \qquad (3)$$

242 Where $q_{e1}$ and $q_t$ refer to the amount of Cr (VI) bio sorbed (mg/g) at equilibrium and at any time,
243 $t$ (min), respectively, and $K_1$ is the equilibrium rate constant of the pseudo-first-order sorption
244 ($min^{-1}$). Equation *3* can be rearranged to obtain a linear form:

$$\ln(q_e - q_t) = \ln q_e - K_1 t \quad (4)$$

The plot of $ln\ (q_e - q_t)$ versus $t$ should give a straight line with slope $-K_1$ and intercept $lnq_e$. $K_1$ and $q_e$, who represented the pseudo-first order constants at different initial Cr (VI) concentration (Table 3). The correlation coefficient value $R^2$ for Cr (VI) bio sorption onto the biomass varied to (0.712 - 0.944). (Fig. 3a) shows a plot of linearized form of pseudo -first order model at different Cr (VI) concentrations.

Table 3: pseudo-first and pseudo-second order kinetic model parameters at different Cr (VI) concentration

| Initial Cr (VI) concentration (mg/l) | Pseudo-first order | | | Pseudo-second order | | | Experimental $q_e$ (mg/g) |
|---|---|---|---|---|---|---|---|
| | $K_1(min^{-1})$ | $q_{e1}$(mg/g) | $R^2$ | $K_2$ (gmg-$^1$min$^{-1}$ | $q_{e2}$(mg/g) | $R^2$ | |
| 10 | 6.7 x 10-3 | 4.27 | 0.948 | 3.9 x 10-3 | 11.61 | 0.977 | 10.74 |
| 20 | 4.8 x 10-3 | 3.34 | 0.963 | 4.4 x 10-3 | 18.66 | 0.999 | 18.68 |
| 40 | 5.1 x 10-3 | 2.75 | 0.747 | 6.3 x 10-4 | 35.97 | 0.994 | 35.78 |
| 80 | 3.8 x 10-3 | 8.42 | 0.712 | 1.8 x 10-3 | 46.30 | 0.1 | 46.03 |

## 2. Pseudo-second order kinetic model

The equation corresponding to the pseudo-second kinetic model is the following (Ho and Mckay 1999):

$$\frac{dq_t}{dt} = K_2(q_e - q_t)2 \quad (5)$$

Integrating this for the boundary condition t = 0, $q_e = 0$, $t = t$, $q_t = q_t$ gives:

$$\frac{1}{q_e - q_t} = \frac{1}{q_e} + K_2 t \quad (6)$$

Where $K_2$ is the equilibrium rate constant of the pseudo-second order biosorption (g/mg$^{-1}$ min$^{-1}$). Eq. *6* can be rearranged to obtain a linear form:

$$\frac{t}{q_t} = \frac{1}{K_2 (q_e)^2} + \frac{1}{q_e} t \quad (7)$$

The equilibrium adsorption capacity and the pseudo-second order constant $K_2$ can be determined experimentally from the slope and the intercept of the plot $t/q_t$ versus $t$. The correlation coefficients calculated were closer to the unity ($R^2$ = 0.977 – 1) and the linear form of the pseudo-second order model was shown in Fig. 3b.

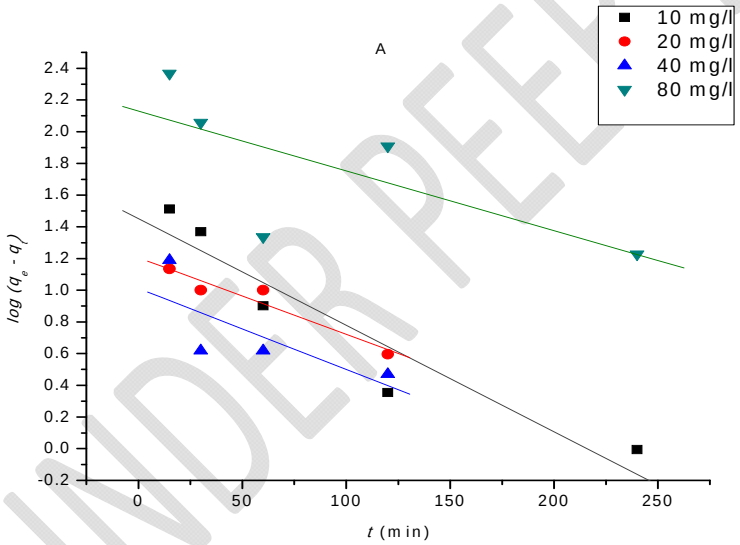

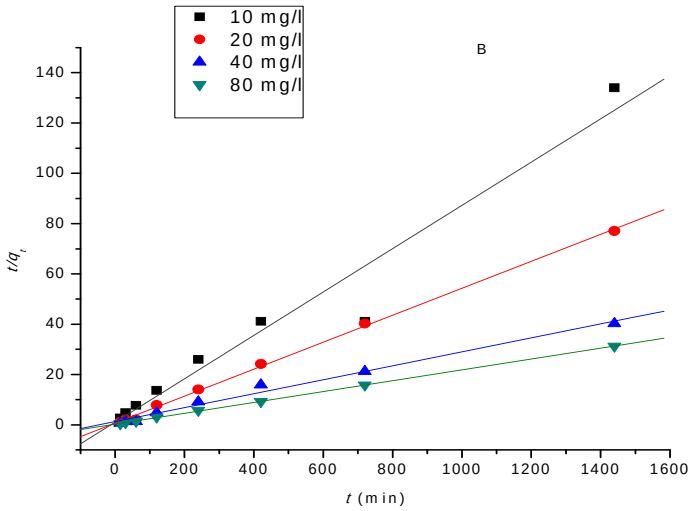


**Fig.3:** Linear form of the pseudo first-order (A) and pseudo second-order (B) models at different Cr (VI) concentration (biomass dosage: 0.05 g/L, pH 2, 100 rpm, and 30˚C)

## 3. Intra-particle diffusion model

The intra-particle diffusion equation is giving as (Cheung et al. 2007):

$$q_t = K_i t^{1/2} + C \quad (8)$$

Where $q_t$ is the amount of solute on the surface of the sorbent at time $t$ (mg/g) and $K_i$ is the intra-particle diffusion rate constant (mg/g min½). When the intra-particle diffusion alone is the rate limiting step, then the plot of $q_t$ versus $t^{1/2}$ passes through the origin. When film diffusion is also taking place then the intercept is $C$, which gives the idea on the thickness of the boundary layer. From the intra-particle diffusion plot shown in (Fig. 4a), it was evident that the adsorption process followed two steps. The first linear portion followed the boundary layer diffusion followed by another linear portion which represents the intra-particle diffusion. This shown that

the adsorption process was not only the intra-particle diffusion but the film diffusion also played a role in the observed process (Vadivelan and Kumar 2005; Nathaji et al. 2013).

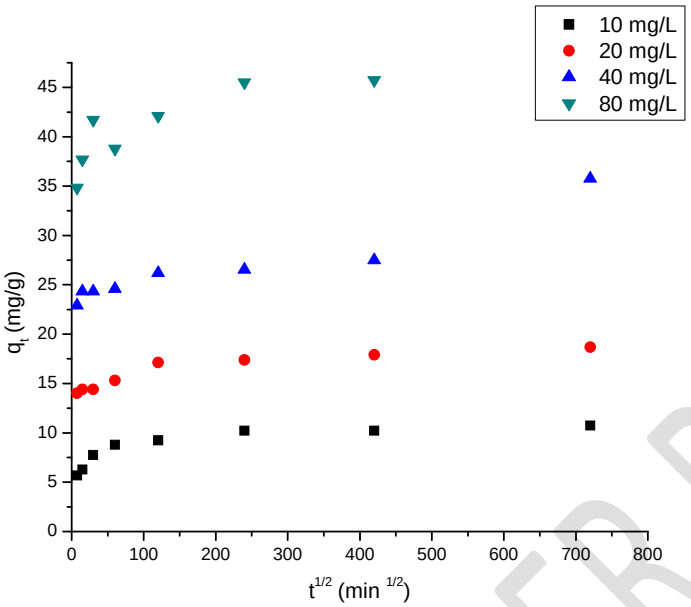


**Fig.4a**: Intra-particle diffusion model for biosorption of Cr (VI) onto *Bacillus cereus* biomass (biosorbent dosage: 0.1 g/L; pH 2; temperature: 30˚ C; agitation: 100 rpm)

## 4. Boyd plot

The Boyd plot predicted the actual slow step involved in the biosorption process. The Boyd kinetic expression is given by (Vadivelan and Kumar 2005):

$$F = 1 - (6/\pi\ (22)^2)\ \exp(-B_t) \quad (9)$$

And

$$F = q_t/q_0 \quad (10)$$

Where $q_0$ is the amount of Cr (VI) adsorbed at infinite time (mg/g) and $q_t$ represents the amount of adsorbent adsorbed at any time $t$ (min), $F$ represents the fraction of solute adsorbed at any time $t$ (min), and $B_t$ is a mathematical function of $F$. substituting *Eq. 9* in *Eq. 10*,

$$1 - F = (6/\pi\ (24)2)\ exp\ (-\ B_t)\ (11)$$

Or

$$B_t = -\ 0.4977 - ln\ (1 - F)\ (12)$$

The $B_t$ values at various contact times can be calculated using *Eq. 12* for various time intervals. The calculated $B_t$ values were plotted against time $t$ (Fig. 4b). It can be shown through the figure that the plots were almost linear for all the concentrations tested.

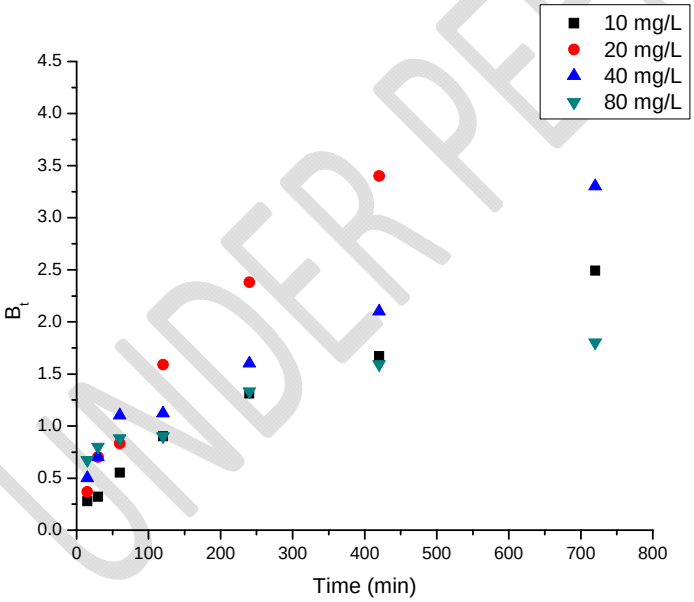


**Fig.4b:** Boyd plot for the biosorption of Cr (VI) onto *Bacillus cereus* biomass (biosorbent dosage: 0.1 g/L; pH 2; temperature: 30˚ C; agitation: 100 rpm)

303 The regression coefficients ($R^2$) calculated for the pseudo-first order equation showing that
304 experimental data do not well agree with the pseudo-first order kinetic model, compare to the
305 pseudo-second order kinetic model. Therefore, the biosorption kinetic could well be
306 approximated more favorable by pseudo-second order kinetic model for Cr (VI) biosorption onto
307 this bacterium biomass. The calculated $q_e$ values from the pseudo-second order equation at
308 different sorbate concentrations were also in good agreement with the experimental values,
309 suggesting that the bio sorption of Cr (VI) ions onto *Bacillus cereus* followed the pseudo-second
310 order kinetic model. It was already demonstrated that the pseudo-second order kinetic equation
311 for adsorption was much similar to the universal rate law for a chemical reaction. Since the
312 processes followed the pseudo-second order equation, it literally suggests that the adsorption was
313 mainly by simple chemical reaction between Cr (VI) ions and the surface functional groups on *B.*
314 *cereus* biomass (Chen et al. 2008; Bennett et al. 2013). The plot of the intra-particle diffusion did
315 not pass through the origin indicating that the adsorption process not only followed the intra-
316 particle diffusion but the film diffusion also played an important role in the adsorption process. It
317 was also in coincidence with the fact that the process followed the pseudo-second order model.
318 The fact that the film diffusion also played a major role in the studied adsorption process
319 suggested that the adsorption was mainly by covalent bonding by the surface acid functional
320 groups. Also the Boyd plot suggested that the rate-determining step is the external mass transfer
321 since the plot was linear and does not pass through the origin.

322 In general the mechanism for metal removal by adsorption/bio adsorption on a sorbent material
323 may be assumed to involve the following four steps: (a) migration of the metal from bulk of the
324 solution to the surface of the adsorbent (bulk diffusion); (b) diffusion of metal through the
325 boundary layer to the surface of the adsorbent (film diffusion); (c) transport of metal from the

surface to the interior pores of the particle (intra-particle diffusion or pore diffusion); (d) adsorption of metal at an active site on the surface of material (chemical reaction via ion-exchange, complexation and/or chelation).

Heavy metal sorption is governed usually by either the liquid phase mass transport rate or the intra-particle mass transport. Hence diffusion mass transport is incorporated into the adsorption process. In diffusion studies, the rate can be expressed in term of the square root time. The mathematical dependence of $q_t$ versus $t^{1/2}$ is obtained if the process is considered to be influenced by diffusion in the particles and convective diffusion in the solution. But from (Fig. 4a), it was evident that the plot did not pass through the origin, this was indicative of some degree of boundary layer control and these further shows that the intra-particle diffusion was not the sole rate controlling step, but other processes may also control the rate of adsorption. From (Fig. 4a), the diffusion mass transfer occurred up to $t^{1/2}$ of around 30 min. This suggests that since chromium is an anionic metal, there was not more intra-particle diffusion due to the presence of some acidic functional groups on the surface of the biomass and hence the adsorption efficiency also decreased accordingly.

It is important to find the slowest step which is the rate-determining step. It was proved by the Boyd plot that external mass transfer is the rate-determining step for the metal. But the extent of the film diffusion and intra-particle diffusion varied based on the ionic nature of the metal [Cr (VI)].

iv. isotherm

346 In this study, the equilibrium data of the biosorption of Cr (VI) ions onto *Bacillus cereus* sorbent
347 at 30˚C were fitted with Langmuir and Freundlich equations.

348 ## 1. Langmuir isotherm

349 Langmuir isotherm is represented by the following equation:

350 $$\frac{1}{q_e} = \frac{1}{q_{max}} + \frac{1}{bq_{max}} \times \frac{1}{C_f} \quad (13)$$

351 The Langmuir's constant *b (L/mg)* and $q_{max}$ were calculated from the initial slope of the linear
352 plot of *1/q* versus $1/C_f$ where *q* and $C_f$ were the adsorption capacities (mg/g) and the final Cr (VI)
353 concentrations (mg/L), respectively. The $q_{max}$ varies from 100 to 25 mg/g at the sorbent dose of
354 0.02 to 0.1g/L, respectively. The regression coefficient ($R^2$) for Langmuir isotherm varies from
355 0.958 to 0.993. The *b* constant for Langmuir varies from 0.01 to 0.04 (Table 4).

356 The essential features of the Langmuir biosorption isotherm can be expressed in term of
357 dimensionless constant called the separation factor or equilibrium parameter (*r*), defined by
358 Weber and Chakkravorti (Kavitha and Namasivayam 2007):

359 $$r = \frac{1}{1+bC_0} \quad (14)$$

360 Where *b* is Langmuir biosorption constant and $C_0$ is the initial Cr (VI) concentration (mg/L).

361 Biosorption is favorable if $0 < r < 1$; unfavorable if $r > 1$; linear if $r = 1$; irreversible if $r = 0$.The ***r*** values
362 for the present study were found to be 0.23 – 0.91 for the initial Cr (VI) concentrations tested.

363 ## 2. Freundlich isotherm

The Freundlich isotherm can be used for non-ideal sorption that involves heterogeneous surface energy systems and is expressed by the following equation:

$$q_e = KC_e e^{\frac{1}{n}} \quad (15)$$

Where $q_e$ refer to amount of Cr (VI) biosorption (mg/g) at equilibrium, $C_e$ is the equilibrium concentration of Cr (VI) in solution (mg/L). Freundlich constant $K$ is a rough indicator of the bio sorption capacity and $1/n$ is the biosorption intensity. In general, as the $K$ value increases the biosorption capacity of a bio sorbent for a given biosorbate increases. *Eq.15* may be linearized by taking logarithms:

$$\log q_e = \log K + \frac{1}{n}\log C_e \quad (16)$$

The plot of $\log C_f$ versus $\log q$ was employed to generate the intercept value of $K$ and the slope of $1/n$. The value of $K$ varies from 3 to 4 and the $n$ values vary from 1.27 to 1.84 (Table 4).

**Table 4**: Langmuir and Freundlich isotherms parameters

| Sorbent (g/l) | Langmuir constants | | | | Freundlich constants | | |
|---|---|---|---|---|---|---|---|
| | $R_2$ | $q_{max}$ (mg/g) | $b$(l/mg) | $q_{e,exp}$ (mg/g) | $R_2$ | $K$ | $N$ |
| 0.02 | 0.978 | 100.3 | 0.01 | 86 | 0.992 | 3 | 1.27 |
| 0.05 | 0.993 | 50.1 | 0.02 | 46 | 0.998 | 4 | 1.68 |
| 0.1 | 0.959 | 25.4 | 0.04 | 29 | 0.986 | 3 | 1.84 |

$q_{e,exp}$: *sorption capacity, experimental values*

377 The regression coefficients ($R^2$) of Langmuir and Freundlich models were greater than 0.9 and
378 were closer to one, indicating that both models adequately described the experimental data. It
379 was obviously that heterogeneous surface conditions co-exist within the monolayer adsorption
380 under the applied conditions. The values calculated from the separation factor (**r**) and the values
381 of Freundlich exponent (*n*), confirmed the favorable sorption process onto the biomass.

382 Previous research showed that Cr (VI) removal capacity of dead *Bacillus licheniformis* was 69.4
383 mg/g (Zhou et al. 2007). Another isolated *Bacillus thuringiensis* has approximately 83.3 mg/g of
384 Cr (VI) biosorption capacity (Sahin and Ozturk 2005). Other research also suggests that the Cr
385 (VI) removal capacity was 70.25 mg/g for *Bacillus cereus* M16 (Subham et al. 2007). Our
386 preliminary research showed that the dried biomass of a facultative anaerobic *Bacillus cereus* Pf-
387 1 was more effective for the removal of Cr (VI) ions from aqueous solution than other *Bacillus*
388 strains previously used (Table 5).

389 **Table 5**: comparison of sorption capacities of the sorbent for the removal of Cr (VI) ions with
390 other *Bacillus* strains

| Metal | Bacterial species | Maximum sorption capacities (mg/g) | References |
|---|---|---|---|
| Cr (VI) | *Bacillus licheniformis* | 69.4 | Zhou et al. 2007 |
| | *Bacillus marisflavi* | 5.783 | Mishra and Doble, 2008 |
| | *Bacillus megaterium* | 30.7 | Srinath et al. 2002 |
| | *Bacillus circulans* | 39.9 | Srinath et al. 2002 |
| | *Bacillus thuringiensis* | 83.3 | Sahin and Ozturk, 2005 |
| | *Bacillus cereus* M16 | 70.25 | Subham et al. 2007 |

| | | | |
|---|---|---|---|
| | *Bacillus cereus* Pf-1 | 100.3 | Present study |
| | *Bacillus phaericus* | 7.62 | Velasquez and Dussan, 2002 |

391

392 ## 4. Conclusion

393 Our results indicated that strain Pf-1 can be potentially used as an efficient biosorbent material
394 compared to other strain of *Bacillus*, because of its remarkable biosorption capacity (100 mg/g)
395 observed during this study. Biosorption data followed the pseudo-second-order kinetic model,
396 suggesting that the rate- limiting step was a chemical biosorption process between Cr (VI) ions
397 and the biomaterial used. Langmuir and Freundlich isotherms adequately described the
398 experimental data indicating that heterogeneous surface conditions might co-exist within the
399 monolayer adsorption under the applied conditions. External mass transfer was the rate-
400 determining step for the adsorption. The adsorption is not only the intra-particle diffusion but the
401 film diffusion also played an important role. The dried biomass of the Pf-1 strain significantly
402 enhanced the biosorption capacity compare to the living or dead biomass previously used. These
403 results show interesting characteristics from the standpoint of biotechnology because the
404 development of a future remediation process using Pf-1 strain can represent an efficient and
405 highly profitable technology for removing the toxic form of Cr.

406 ## 5. References

407 Abbas M, Nadeem R, Nadeem MZ, Arshad M (2008) Biosorption of chromium (III) and
408 chromium (VI) by untreated and pretreated *Cassia fistula* biomass from aqueous solutions.
409 Water Air Soil Pollut 191: 139-148

410 Ashkenazy R, Gottlieb L, Yannai S (1997) Characterization of acetone washed yeast biomass
411 functional groups involved in lead biosorption. Biotechnol Bioeng 55:1–10

412 APHA (American Public Health Association); American Water Works Association (AWWA);
413 Water Environment Federation (WEF) (1995) Standard Methods for the Examination of Water
414 and Wastewater, 19th ed. Washington, DC

415 Aliabadi M, Khazaei I, Fakhraee H (2012) Hexavalent chromium removal from aqueous
416 solutions by using low-cost biological wastes: equilibrium and kinetic studies. Int J Environ Sci
417 Technol 9: 319-326

418 Bennett R, Cordero F, Bautista S, Dedeles R (2012) Reduction of hexavalent chromium using
419 fungal and bacterial isolated from contaminated soil and water samples, Chemistry and Ecology
420 29: 320-328

421 Beveridge TJ, Murray RGE (1980) Sites of metal deposition in the cell wall of Bacillus subtilis. J
422 Bacteriol 141:876–887

423 Chen WM., Wu CH, Euan KJ, Jo-Shu C (2008) Metal biosorption capability of *Cupriavidus*
424 *taiwanensis* and its effects on heavy metal removal by nodulated Mimosa pudica, J Hazard Mater
425 151: 364-371

426 Cheung WH, Szeto YS, McKay G (2007) Intraparticle diffusion processes during acid dye
427 adsorption onto chitosan. Bioresour Technol 98: 2897-2904

428 Giri AK, Patel RK, Mahapatra SS, Mishra PC (2013) Biosorption of Arsenic (III) from aqueous
429 solution by living cells of *Bacillus cereus.* Environ Sci Pollut Res 20: 1281-1291

Fernandez PM, Cruz EL, Vinarta SC, Figueroa LI (2017) optimization of culture condition for growth associated with Cr (VI) removal by Wickerhamomyces anomalus M10. Bull Environ Contam Toxicol 98:400-406

Fernandez PM, Cruz EL, Vinarta SC, Figueroa LI (2018). Bioremediation strategies for chromium removal: current research, scale-up approach and future perspectives. Chemosphere. 208:139-148

Giri AK, Patel RK, Mahapatra SS (2011) Artificial neural network (ANN) approach for modeling of arsenic (III) biosorption from aqueous solution by living cells of *Bacillus cereus* biomass. Chemical Eng J 178: 15-25

Ho YS, Mckay G (1999) Pseudo second order model for sorption processes. Process Biochem 34: 451-465.

Kavitha D, Namasivayam C (2007) Experimental and kinetic studies on methylene blue adsorption by coir pith carbon. Bioresour Technol 98: 14-21

Kamnev AA (2008) FTIR spectroscopic studies of bacterial cellular responses to environmental factors, plant-bacterial interactions and signalling. Spectroscopy 22:83–95

Kang SY, Bremer PJ, Kim KW, McQuillan AJ (2006) Monitoring metal ion binding in single-layer *Pseudomonas aeruginosa* biofilms using ATR-IR spectroscopy. Langmuir 22:286–291

Mishra S, Doble M (2008) Novel chromium tolerant microorganisms: isolation, characterization and their biosorption capacity. Ecotox Environ Safe 71: 874-879.

449 Mufedah AH, Gazem Sarita N (2012) Isotherm and kinetic models and cell surface analysis for
450 determination of the mechanism of metal sorption by *Aspergillus versicolor.* World J Microbiol
451 Biotechnol 28: 2521-2530.

452 Naik UC, Srivastava S, Thakur IS (2012) Isolation and characterization of *Bacillus cereus*
453 IST105 from electroplating effluent for detoxification of hexavalent chromium. Environ Sci
454 Pollut Res 19:3005-3014

455 Nethaji S, Sivasamy A, Mandal AB (2013) Adsorption isotherms, kinetics and mechanism of the
456 adsorption of cationic and anionic dyes onto carbonaceous particles prepared from *Juglans regia*
457 shell biomass. Int J Environ Sci and Technol 10: 231-242

458 Nguema PF, Luo Z, Lian JJ (2014) The biosorption of Cr (VI) ions by dried biomass obtained
459 from a chromium-resistant bacterium. Front. Chem Sci Eng DOI 10.1007/s11705-014-1456-4

460 Qing H, Hongyan Q, Zhihui B, Minna D, Jinghai Z, Fanyuanghang Z, Hongxun Z (2007)
461 Biosorption of Cadmium by a $Cd^{2+}$ hyperresistant *Bacillus cereus* strain HQ-1 newly isolated
462 from a lead and zincs mine. World J Microbiol Biotechnol 23: 971-976

463 Reya I, Rajamehala M, Lakshmi M, Emillin R (2012) Comparative study on biosorption of
464 hexavalent chromium using Aspergilus oryzae NCIM 637 and Aspergilus sojae NCIM 1198
465 from electroplating effluent. Int J Chemistry Technol Res 4: 1708-1719

466 Rabei Sanna MG, Gad-Elrab MF, Romany NN, Abskharon Sedky AH, Shoreit AM (2009)
467 Biosorption of hexavalent chromium using biofilm *E. coli* supported on granulated activated
468 carbon. World J Microbiol Biotechnol 25: 1695-1703

469 Stenfors Arnesen LP, Fagerlund A, Granum PE (2008) From soil to gut: *Bacillus cereus* and its
470 food poisoning toxins. FEMS Microbiol Rev 32: 579-606.

471 Srinath T, Verma T, Ramteke PW, Garg SK (2002) Chromium (VI) biosorption and
472 bioaccumulation by chromate resistant bacteria. Chemosphere 48: 427-35

473 Şahin Y, Öztürk A (2005) Biosorption of chromium (VI) ions from aqueous solution by the
474 bacterium *Bacillus thuringiensis*. Process Biochem 40: 1895-901

475 Subham P, Debabrata B, Parimal C, Lalitagauri R (2007) Biosorption of Cr (VI) by a mutated
476 strain of *Bacillus cereus* M16, J Hazard Subst Res 7

477 Srivastava S, Thakur S (2006) Evaluation of bioremediation and detoxification potentiality of
478 *Aspergillus niger* for removal of hexavalent chromium in soil microcosm. Soil Biology Biochem
479 38: 1904-1911.

480 Samuel J, Paul ML, Pulimi M, Nirmala MJ, Chandrasekaran N, Mukherjee A (2012) Hexavalent
481 chromium bioremoval through adaptation and consortia development from sukinda chromite
482 mine isolates, Industrial Eng Chemistry Res 51: 3740-3749.

483 Sivasamy A, Sundarabal N (2011) Biosorption an Azo dye by *Aspergillus niger* and
484 *Trichoderma sp*. Fungal biomasses. Curr Microbiol 62: 351-357

485 Velasquez L, Dussan J (2009) Biosorption and bioaccumulation of heavy metals on dead and
486 living biomass of *Bacillus sphaericus.* J Hazard Mater 167: 713-716

487 Vadivelan V, Vasanth Kumar K (2005) Equilibrium, kinetics,mechanism, and process design for
488 the sorption of methylene blue onto rice husk . J Colloid Interface Sci 286: 90-100

489 Zhou M, Liu Y, Zeng G, Li X, Xu W, Fan T (2007) Kinetic and equilibrium studies of Cr (VI)
490 biosorption by dead *Bacillus licheniformis* biomass. World J Microbiol Biotechnol 23**:** 43-48

491 Zhu Y, Zhang H, Zeng H, Liang M, Lu R (2012) Adsorption of chromium (VI) from aqueous
492 solution by the ion (III)-impregnated sorbent prepared from sugarcanes bagasse. Int J Environ
493 Sci Technol 9: 463-472

494

495

496